Influence of pump intensity on atomic spin relaxation in a vapor cell*

Chen Yang(杨晨)[1,2], Guan-Hua Zuo(左冠华)[1,2], Zhuang-Zhuang Tian(田壮壮)[1,2], Yu-Chi Zhang(张玉驰)[3,†], and Tian-Cai Zhang(张天才)[1,2,‡]

[1] State Key Laboratory of Quantum Optics and Quantum Optics Devices, Institute of Opto-Electronics, Shanxi University, Taiyuan 030006, China
[2] Collaborative Innovation Center of Extreme Optics, Shanxi University, Taiyuan 030006, China
[3] College of Physics and Electronics Engineering, Shanxi University, Taiyuan 030006, China

(Received 23 August 2019; revised manuscript received 29 September 2019; published online 25 October 2019)

Atomic spin relaxation in a vapor cell, which can be characterized by the magnetic resonance linewidth (MRL), is an important parameter that eventually determines the sensitivity of an atomic magnetometer. In this paper, we have extensively studied how the pump intensity affects the spin relaxation. The experiment is performed with a cesium vapor cell, and the influence of the pump intensity on MRL is measured at room temperature at zero-field resonance. A simple model with five atomic levels of a Λ-like configuration is discussed theoretically, which can be used to represent the experimental process approximately, and the experimental results can be explained to some extent. Both the experimental and the theoretical results show a nonlinear broadening of the MRL when the pump intensity is increasing. The work helps to understand the mechanism of pump induced atomic spin relaxation in the atomic magnetometers.

Keywords: atomic magnetometer, atomic spin relaxation, optical pumping

PACS: 76.60.Es, 78.20.Ls, 33.57.+c, 32.80.Xx **DOI:** 10.1088/1674-1056/ab4cde

1. Introduction

Atomic magnetometry[1,2] has been extensively investigated in the past decades. The sensitivity of atomic magnetometry is related to the spin relaxation and it can be measured by observing the change of atomic polarization in a magnetic field.[3] In this measurement, optical pumping is necessary to generate the atomic polarization[4] through the absorption–emission cycle of atom–light interaction,[5,6] and such optical pumping process has been considered as one of the fundamentals of magnetic field measurement.[7,8] The atomic spin relaxation time T_2 in the vapor cell is a very important parameter which directly determines the sensitivity of an atomic magnetometer.[9–11] The spin relaxation in the vapor cell is affected by many factors, such as diffusion of atoms,[12,13] collision between atoms,[14–16] optical pumping, etc. The relaxation caused by diffusion and collision can be suppressed by some advanced techniques, such as atom-relaxation coating of the vapor cell,[17] optimizing the filling of buffer gas,[18] controlling the temperature of the vapor cell,[19] reducing the magnetic field gradient,[20] etc. The relaxation caused by optical pumping can be controlled by optimizing the pump intensity,[21] which is inevitable and cannot be eliminated completely.

The atomic spin relaxation time T_2 is characterized by the magnetic resonance linewidth (MRL) of the light-induced magnetic resonance $\Delta\omega$ ($\Delta\omega = 1/T_2$).[10,22] By observing the atomic polarization in different magnetic field around zero-point (so called zero-field resonance),[23] or by tuning the modulation frequency of the pump beam around the magnetic resonance frequency,[24–26] the magnetic resonance spectrum (MRS) can be measured. For a linear pump, the magnetic resonance frequency is equal to twice of the Larmor frequency ($2\omega_L$).[27,28] The magnetic resonance process can be treated by Bloch equations and the MRS can be figured out which is normally a Lorentzian shape,[29] from which the MRL (the half width at half maximum of MRS) is obtained.[30]

Usually, the MRL can simply be treated as linear broadening[22,31] with the increase of the pump intensity. However this treatment is actually incomplete. In 1999, the nonlinear light narrowing was investigated theoretically and experimentally,[21] and the nonlinear broadening was also analyzed later[32] based on a simplified ideal atomic system. By solving the Liouville equation with an unmodulated pump beam, the nonlinear broadening was obtained. Recently, Han *et al.* finished the experimental testing of pump induced nonlinear broadening in a heated rubidium vapor cell, in which the circularly polarized pump beam was amplitude modulated.[33]

In this paper, we have investigated the influence of the pump intensity on spin relaxation at room temperature. The experiment is performed with a cesium vapor cell with buffer gas, and an unmodulated linear polarized pump beam locked to the D_1 line of cesium is used. The MRL is measured with the probe beam tuned on resonance to the D_2 transition. The MRL is measured at zero-field resonance, and the results show that the relation between MRL and pump intensity is nonlinear

*supported by the National Key R&D Program of China (Grant No. 2017YFA0304502) and the National Natural Science Foundation of China (Grant Nos. 11634008, 11674203, 11574187, and 61227902).

†Corresponding author. E-mail: yczhang@sxu.edu.cn
‡Corresponding author. E-mail: tczhang@sxu.edu.cn

broadening. To the best of our knowledge, this is the first time this phenomenon is observed experimentally. We have also used a simplified five-level atomic system model with one excited state and four ground states to represent our experimental configuration, and by solving the Liouville equation,[34,35] the experimental result can be explained approximately.

2. Experimental setup and results

The experiment for testing the influence of the pump intensity on atomic spin relaxation is carried out at room temperature (~ 25 ℃), and the experimental setup is shown in Fig. 1. The system includes three parts: the vapor cell, the laser system, and the detection system.

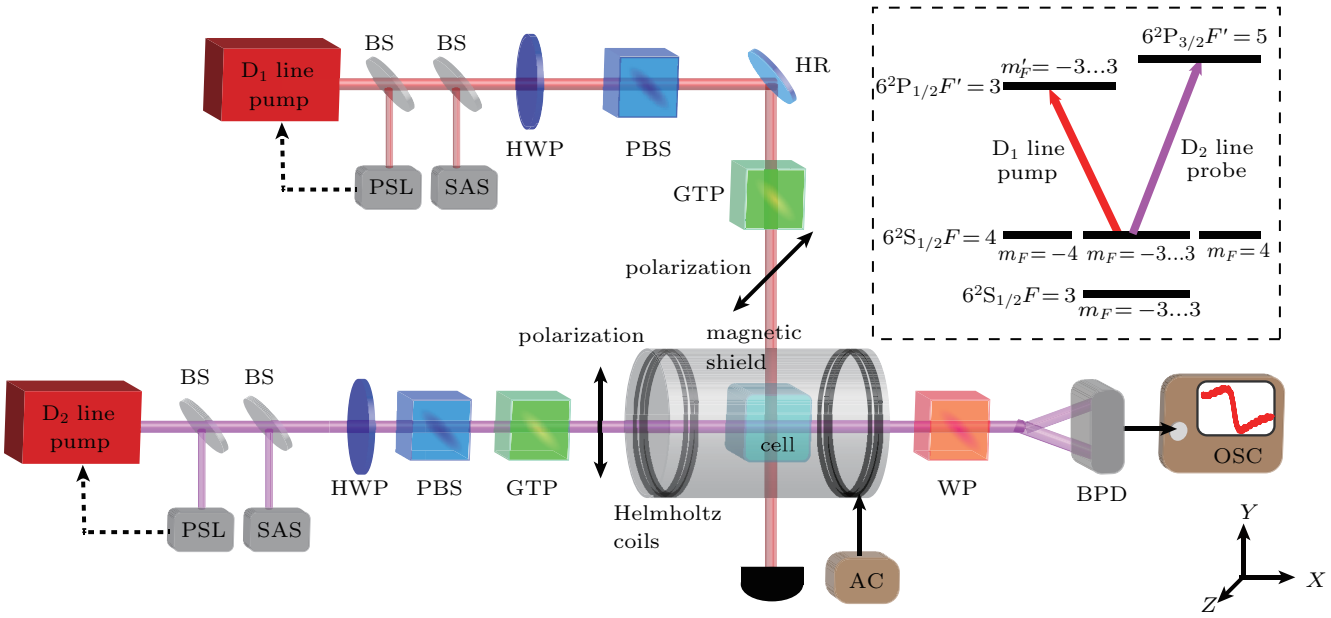

Fig. 1. Experimental setup for measuring the MRL. BS: beam splitter; PSL: the laser frequency control system by polarization spectrum locking technique; SAS, saturated absorption spectrum; HWP, half-wave plate; PBS, polarization beam splitter; HR, highly reflective mirror; GTP, Glan–Taylor prism; WP, Wollaston prism; BPD, balanced photodetector; AC, alternating current power supply; OSC, oscilloscope. The involved energy levels of cesium atom are shown in the upper right. m_F and m'_F denote the magnetic quantum numbers of the ground and excited states, respectively. The Z polarized pump beam and the Y polarized probe beam are resonance to cesium D_1 line $6^2S_{1/2}F = 4$ to $6^2P_{1/2}F' = 3$ and D_2 line $6^2S_{1/2}F = 4$ to $6^2P_{3/2}F' = 5$, respectively. The magnetic field (along the X direction) can be changed near the zero point by sweeping the driving current of the Helmholtz coil via AC, and the MRL can be obtained via OSC.

The vapor cell The cesium vapor cell has dimensions of 20 mm×20 mm×20 mm, and contains 20 Torr of helium as a buffer gas. The cell is put into a magnetic field along the X direction that is created by a pair of Helmholtz coils, which is driven by an alternating current power supply (AC, SRS DS335). The entire system is set in a magnetic shield cylinder, in which the residual magnetism is less than 2 nT.

The laser system The pump laser is polarized along the Z direction, and it is tuned to resonant to the cesium D_1 transition $6^2S_{1/2}F = 4$ to $6^2P_{1/2}F' = 3$. The probe laser is polarized along the Y direction with a fixed intensity of 0.02 mW/cm^2, and the probe frequency is locked to the cesium D_2 line $6^2S_{1/2}F = 4$ to $6^2P_{3/2}F' = 5$. Here, F and F' represent the atomic total angular momenta of the ground and excited states, respectively.

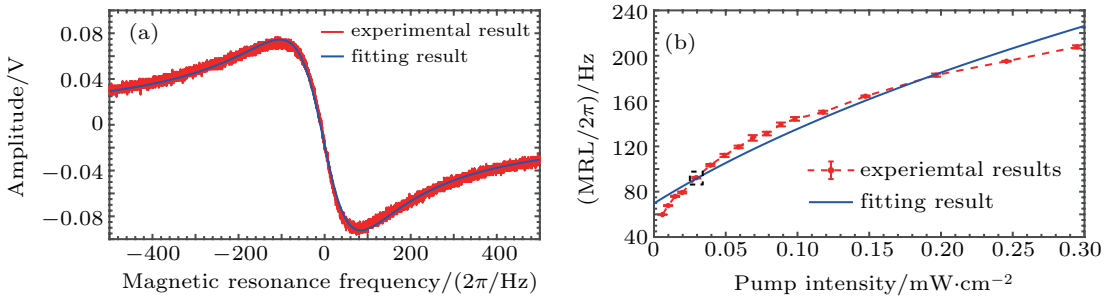

Fig. 2. Experimental results for measuring the MRL. (a) MRS for a fixed pump intensity of 0.03 mW/cm^2. The MRS is shown as the output of the balanced photodetector as a function of the magnetic resonance frequency $2\omega_L = 2\gamma B$, where $\gamma = 2\pi \times 3.5$ Hz/nT for the ground state of the cesium atom. The MRS is fitted by the dispersive Lorentzian shape (blue line, the red line is the experimental result), and the MRL is figured out as $\Delta\omega = 2\pi \times (93.5 \pm 0.1)$ Hz (see the point with a black dotted cycle in (b)). (b) Relation between MRL and pump intensity. The red dots are the experimental results and the solid blue line is the theoretical fitting according to Eq. (12) (see the theoretical discussion below). Nonlinear relation is clearly shown and each data point and the error bar are obtained from five measurements. The best fitting gives the following parameters: $\alpha = 2\pi \times (2.1 \pm 0.2) \times 10^3$ Hz·cm^2/mW and $r_0 = 2\pi \times (69.7 \pm 4.4)$ Hz.

The detection system The polarization of the probe beam transmitted through the vapor cell is detected by a balanced polarimeter, which is formed by a Wollaston prism (WP) and a balanced photodetector (BPD, New Focus 2307). The MRS of zero-field resonance for a fixed pump intensity can be measured by sweeping the magnetic field around the zero point (as shown in Fig. 2(a)), the MRS can be fitted by the dispersive Lorentzian shape, then the MRL can be obtained.

The dependence of MRL on the pump intensity is shown in Fig. 2(b). The red dots are the experimental results. Nonlinear broadening is clearly shown in the entire pump range, which is indeed quite different from the usual simple linear explanation and treatment,[22] as mentioned above. The blue line in Fig. 2(b) is the theoretical fitting according to Eq. (12) and it agrees with the experiment results in some extent. We are going to discuss it below.

3. Theoretical model and analysis

In this part, we are trying to give an explanation to the above observed results. As shown in Fig. 1, if we consider the interaction between cesium D_1 transition and linearly polarized pump beam, there are totally 23 Zeeman sublevels involved, which are too complex to be solved. The process can actually be simplified to a five-level system as shown in Fig. 3. The reasons are list as follows.

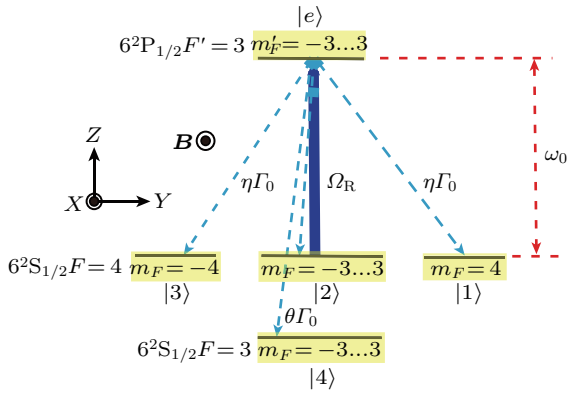

Fig. 3. Simplified five-level configuration. The Zeeman sublevels in ground state $6^2S_{1/2}F=4$ are represented by three states:$|1\rangle$, $|2\rangle$, and $|3\rangle$, and state $|4\rangle$ represents the other ground state $6^2S_{1/2}F=3$. A resonance pump light linearly polarized along the Z direction couples ground state $6^2S_{1/2}F=4$ and the excited state $6^2P_{1/2}F'=3$ (represented by $|e\rangle$) with Rabi frequency Ω_R. The total spontaneous decay rate of $|e\rangle$ is $\Gamma_0=2\pi\times4.5\times10^6$ Hz for cesium. The decay rates of $|e\rangle$ to $|1\rangle$ and $|3\rangle$ are defined as $\eta\Gamma_0$, while the rate from $|e\rangle$ to $|4\rangle$ is $\theta\Gamma_0$. The direction of the magnetic field is along the X direction.

(I) Since all the Zeeman sublevels in excited state $6^2P_{1/2}F'=3$ are involved in the optical pumping process, and all these Zeeman sublevels have the same spontaneous decay rate Γ_0[6] (for cesium, $\Gamma_0=2\pi\times4.5\times10^6$ Hz), we can treat all these seven sublevels as one state $|e\rangle$.

(II) The Zeeman sublevels in ground state $6^2S_{1/2}F=4$ are separated into two parts: the first part is the Zeeman sublevels involved in the optical pumping process, corresponding to $-3\leqslant m_F\leqslant3$, and this part can be represented as state $|2\rangle$. The second part is the rest of the Zeeman sublevels, corresponding to $m_F=4$ and $m_F=-4$, which can be represented as states $|1\rangle$ and $|3\rangle$, respectively.

(III) The ground state $6^2S_{1/2}F=3$ is not involved in the optical pumping process, but some of the atoms still fall into this ground state through spontaneous emission process from the excited state $6^2P_{1/2}F=3$, so we can represent these Zeeman sublevels as one state $|4\rangle$.

Since we have simplified our atomic level system, the spontaneous decay rate from excited state $|e\rangle$ to each ground state $|1\rangle$, $|2\rangle$, and $|3\rangle$ must be modified. We use $\eta\Gamma_0$ and $\theta\Gamma_0$ to represent the recalculated spontaneous decay rates from $|e\rangle$ to balanced states ($|1\rangle$ and $|3\rangle$) and state $|4\rangle$, respectively. η and θ can be estimated by using the dipole matrix elements[36]

$$\eta=\frac{(D_{F=4,m_F=4}^{F'=3,m'_F=3})^2}{\sum\limits_{m'=-3}^{3}\sum\limits_{f=3}^{4}\sum\limits_{m=-f}^{f}(D_{F=f,m_F=m}^{F'=3,m'_F=m'})^2},$$
$$\theta=\frac{\sum\limits_{m'=-3}^{3}\sum\limits_{m=-3}^{3}(D_{F=3,m_F=m}^{F'=3,m'_F=m'})^2}{\sum\limits_{m'=-3}^{3}\sum\limits_{f=3}^{4}\sum\limits_{m=-f}^{f}(D_{F=f,m_F=m}^{F'=3,m'_F=m'})^2}, \quad (1)$$

where $D_{F=f,m_F=m}^{F'=3,m'_F=m'}$ represents the dipole matrix elements between the Zeeman sublevels in ground state $6^2S_{1/2}F=f$ with $m_F=m$ and the Zeeman sublevel in excited state $6^2P_{1/2}F'=3$ with $m'_F=m'$; for cesium, $\eta=0.08$ and $\theta=0.25$.

As shown in Fig. 3, the resonance pump light with linear polarization along Z direction couples $|2\rangle$ and $|e\rangle$ with Rabi frequency Ω_R, and the magnetic field is along the X direction. We choose Z direction as the quantization axis, and the time evolution of the density matrix $\hat{\rho}$ of the system is given by the Liouville equation[34]

$$i\hbar\frac{d}{dt}\hat{\rho}=[\hat{H},\hat{\rho}]-i\hbar\frac{1}{2}(\hat{\Gamma}\hat{\rho}+\hat{\rho}\hat{\Gamma})+i\hbar\hat{\Lambda}, \quad (2)$$

where $\hbar$ is the reduced Planck constant. The total Hamiltonian $\hat{H}$ consists of three parts

$$\hat{H}=\hbar\omega_0|e\rangle\langle e|+\hbar\Omega_R\cos(\omega_0 t)(|2\rangle\langle e|+|e\rangle\langle 2|)+\hbar\omega_L\hat{F}_x. \quad (3)$$

The first part represents the free atomic energy, and the second and third parts are the Hamiltonians of the atom–pump light interaction and atom–magnetic field coupling, respectively. ω_0 is the transition frequency between $|2\rangle$ and $|e\rangle$. $\hat{F}_x$ is the angular momentum operator along the X direction and $\omega_L=\gamma B$ is the Larmor frequency with γ being the gyromagnetic ratio.

The second and third terms in Eq. (2) represent the depopulation ($\hat{\Gamma}$) and repopulation ($\hat{\Lambda}$) of the ground and excited states without the influence of pump light and magnetic field, respectively. It should be mentioned that in the absence of the pump beam, the relaxation rates of the Zeeman sublevels are

different due to spin exchange collisions.[37] In our model, for the sake of simplicity, we consider the same relaxation rate, represented as r_0. Under this condition, depopulation and repopulation should be

$$\begin{aligned}\hat{\Gamma} &= r_0(|1\rangle\langle 1|+|2\rangle\langle 2|+|3\rangle\langle 3|+|4\rangle\langle 4|)\\ &\quad+(r_0+\Gamma_0)|e\rangle\langle e|, \qquad (4)\\ \hat{\Lambda} &= \frac{1}{4}r_0(|1\rangle\langle 1|+|2\rangle\langle 2|+|3\rangle\langle 3|+|4\rangle\langle 4|)\\ &\quad+[\eta(|1\rangle\langle 1|+|3\rangle\langle 3|)+(1-2\eta-\theta)|2\rangle\langle 2|\\ &\quad+\theta|4\rangle\langle 4|]\Gamma_0\rho_{ee}. \qquad (5)\end{aligned}$$

In the rotating-wave approximation, the steady-state solutions of Eq. (2) can be obtained. The solution of the elements of the density matrix has a symmetric form

$$\rho_{11}=\rho_{33},\quad \rho_{32}=\rho_{12}=\rho_{21}^{*}=\rho_{23}^{*},\quad \rho_{13}=\rho_{31}, \qquad (6)$$

which means that the atomic polarization in $6^2S_{1/2}F=4$ is anti-symmetric in both the Y and Z axes.[4]

A probe beam is used to detect the component of the atomic polarization in $6^2S_{1/2}F=4$ along the Y direction, which can be expressed by an operator $\hat{P}_y$. From the symmetry shown in relation (6), $\hat{P}_y$ can be considered as a combination of the atomic polarizations in state $6^2S_{1/2}F=4$ along the positive Y direction ($\hat{P}_{y+}$) and negative Y direction ($\hat{P}_{y-}$)[38]

$$\hat{P}_y=\hat{P}_{y+}-\hat{P}_{y-}=\begin{pmatrix}\sigma_y & 0\\ 0 & 0\end{pmatrix}-\begin{pmatrix}0 & 0\\ 0 & \sigma_y\end{pmatrix}=\begin{pmatrix}0 & -\mathrm{i} & 0\\ \mathrm{i} & 0 & \mathrm{i}\\ 0 & -\mathrm{i} & 0\end{pmatrix}, \qquad (7)$$

where σ_y is the Pauli matrix along the Y direction. What we have measured in experiment is $\langle\hat{P}_y\rangle$,[35] which is

$$\langle\hat{P}_y\rangle=\mathrm{Tr}(\hat{\rho}_0\hat{P}_y), \qquad (8)$$

where $\hat{\rho}_0$ is the density matrix of state $6^2S_{1/2}F=4$

$$\hat{\rho}_0=\begin{pmatrix}\rho_{11} & \rho_{12} & \rho_{13}\\ \rho_{21} & \rho_{22} & \rho_{23}\\ \rho_{31} & \rho_{32} & \rho_{33}\end{pmatrix}. \qquad (9)$$

Usually, Γ_0 is much larger than r_0, and if we consider the case of the near-zero magnetic field, the Larmor frequency ω_{L} is on the order of r_0. In this situation, we can define a normalized Larmor frequency parameter $u=2\omega_{\mathrm{L}}/r_0$. $\langle\hat{P}_y\rangle$ can then be expressed as

$$\begin{aligned}\langle\hat{P}_y\rangle &= 2\mathrm{i}(\rho_{12}-\rho_{21})\\ &= \frac{-(3\eta+\theta)ku}{\sqrt{2}[(\eta k+\theta k+2)u^2+(2\eta+\theta)k^2+(4\eta+2\theta+1)k+2]}.\end{aligned} \qquad (10)$$

Here, the optical-pumping saturation parameter k is proportional to the pump intensity[34]

$$k=\alpha I_0/r_0, \qquad (11)$$

where I_0 is the pump intensity and $\alpha=\Omega_{\mathrm{R}}^2/(I_0\Gamma_0)$.

The dependence of $\langle\hat{P}_y\rangle$ on the parameter u with certain pump intensity has a dispersive Lorentzian shape, and its half width at half maximum Δu is directly proportional to the MRL $\Delta\omega=\Delta u\times r_0$. Thus, $\Delta\omega$ can be expressed as

$$\Delta\omega=r_0\sqrt{\frac{(2\eta+\theta)k^2+(4\eta+2\theta+1)k+2}{k(\eta+\theta)+2}}. \qquad (12)$$

We can see that, in general, the relation between MRL and pump intensity is not linear in the whole range of pump. The fitting of the experimental results is shown as the solid blue line in Fig. 2(b), which explains the nonlinear broadening to some extent. The discrepancy between theory and experiment is due to the simplified model in which the isotropic spin relaxation has been assumed.

4. Conclusion

We have investigated the influence of the pump intensity on atomic spin relaxation. The spin relaxation is characterized by the MRL. The experiment is performed in a cesium vapor cell with 20 Torr helium as a buffer gas at room temperature. The nonlinear broadening of MRL along with the pump intensity increasing is observed. A simplified five-level atomic configuration is analyzed which can represent our experiment system to a certain extent, and the dependence of the MRL on pump intensity is obtained theoretically. The nonlinear relation between MRL and pump intensity is expected, which explains our experimental results to some extent. The reported results provide a better understanding of the atom–field interaction in atomic magnetometers.

Appendix A: Solution of the Liouville equation

The density matrix ρ in Eq. (2) can be expressed as

$$\rho=\begin{pmatrix}\rho_{11} & \rho_{12} & \rho_{13} & \rho_{14} & \rho_{1e}\\ \rho_{21} & \rho_{22} & \rho_{23} & \rho_{24} & \rho_{2e}\\ \rho_{31} & \rho_{32} & \rho_{33} & \rho_{34} & \rho_{3e}\\ \rho_{41} & \rho_{42} & \rho_{43} & \rho_{44} & \rho_{\rho_{4e}}\\ \rho_{e1} & \rho_{e2} & \rho_{e3} & \rho_{e4} & \rho_{ee}\end{pmatrix}. \qquad (A1)$$

Combing Eqs. (2)–(5) and (A1), and replacing the pump intensity I_0 and Larmor frequency ω_{L} with the optical-pumping saturation parameter k and normalized Larmor frequency parameter u, we can obtain the elements of the density matrix ρ_0, which obey the relation shown in Eq. (6):

$$\begin{aligned}\rho_{11}=\rho_{33}=\frac{1}{8A}\times\{&4r^3\left(4+5u^2+u^4\right)\\ &+r^2\Gamma[5k\left(4+u^2\right)+4\left(8+9u^2+u^4\right)]\\ &+2r\Gamma^2[2k^2+10\left(1+u^2\right)+k\left(7+u^2+12\eta+4\theta\right)]\\ &+\Gamma^3[4\left(1+u^2\right)+2k^2\left(3\eta+\theta\right)\\ &+k\left(2+3\left(4+u^2\right)\eta+\left(4+u^2\right)\theta\right)]\},\end{aligned}$$

$$\rho_{22}=\frac{1}{4A}\times\{2r^3\left(4+5u^2+u^4\right)+r^2\Gamma[3k\left(2+u^2\right)+2\left(8+9u^2+u^4\right)]+\Gamma^3\left(2+k+2u^2\right)+r\Gamma^2[k^2+10\left(1+u^2\right)+k\left(5-u^2\left(-2+3\eta+\theta\right)\right)]\},$$

$$\rho_{32}=\rho_{12}=\rho_{21}^*=\rho_{23}^*=\frac{\mathrm{i}}{4\sqrt{2}A}\times\{ku[3r^2\Gamma+\Gamma^3\left(3\eta+\theta\right)+2r\Gamma^2\left(1+3\eta+\theta\right)]\},$$

$$\rho_{13}=\rho_{31}=\frac{-1}{8A}\times\{ku^2[3r^2\Gamma+\Gamma^3\left(3\eta+\theta\right)+2r\Gamma^2\left(1+3\eta+\theta\right)]\}, \tag{A2}$$

where parameter A is

$$A=2r^3\left(4+5u^2+u^4\right)+2r^2\Gamma[8+9u^2+u^4+k\left(5+2u^2\right)]+\Gamma^3[2\left(1+u^2\right)+k^2\left(2\eta+\theta\right)+k\left(1+\left(4+u^2\right)\eta+\left(2+u^2\right)\theta\right)]+r\Gamma^2[2k^2+10\left(1+u^2\right)+k\left(7+8\eta+4\theta+u^2\left(2-\eta+\theta\right)\right)]. \tag{A3}$$

Then $\langle\hat{P}_y\rangle$ (see Eq. (8)) can be expressed as

$$\langle\hat{P}_y\rangle=2\mathrm{i}(\rho_{12}-\rho_{21})=\frac{-1}{\sqrt{2}A}\times\{ku[3r^2\Gamma+\Gamma^3\left(3\eta+\theta\right)+2r\Gamma^2\left(1+3\eta+\theta\right)]\}. \tag{A4}$$

The expression of $\langle\hat{P}_y\rangle$ looks very complicated, but under the condition of $\Gamma_0\gg r_0$, the expression can be much simpler, as shown in Eq. (10).

References

[1] Budker D and Romalis M 2007 *Nat. Phys.* **3** 227
[2] Degen C L, Reinhard F and Cappellaro P 2018 *Rev. Mod. Phys.* **89** 035002
[3] Bloom A L 1962 *Appl. Opt.* **1** 61
[4] Rochester S M and Budker D 2001 *Am. J. Phys.* **69** 450
[5] Happer W 1973 *Rev. Sci. Instrum.* **44** 169
[6] Happer W 1973 *Rev. Mod. Phys.* **44** 169
[7] Kitching J, Knappe S and Donley E A 2011 *IEEE Sens. J.* **11** 1749
[8] Zhang J H, Liu Q, Zeng X J, Li J X and Sun W M 2012 *Chin. Phys. Lett.* **29** 068501
[9] Ranjbaran M, Tehranchi M M, Hamidi S M and Khalkhali S M H 2019 *J. Magn. Magn. Mater.* **469** 522
[10] Grosz A, Mukhopadhyay S C and Haji-Sheikh M J 2017 *High Sensitivity Magnetometers (Smart Sensors, Measurement And Instrumentation)* (Switzerland: Springer International Publishing) p. 429
[11] Ding Z C, Yuan J, Wang Z G, Yang K Y and Luo H 2015 *Chin. Phys. B* **24** 083202
[12] Franzen W 1959 *Phys. Rev.* **115** 850
[13] Hasson K C, Cates G D, Lerman K, Bogorad P and Happer W 1990 *Phys. Rev. A* **41** 3672
[14] Franz F A and Sooriamoorthi C E 1974 *Phys. Rev. A* **10** 126
[15] Bhaskar N D, Pietras J, Camparo J, Happer W and Liran J 1980 *Phys. Rev. Lett.* **44** 930
[16] Beverini N, Minguzzi P and Strumia F 1971 *Phys. Rev. A* **4** 550
[17] Seltzer S J, Rampulla D M, Rivillon-Amy S, Chabal Y J, Bernasek S L and Romalis M V 2008 *J. Appl. Phys.* **104** 103116
[18] Gao Y, Dong H F, Wang X, Wang X F and Yin L X 2017 *Chin. Phys. B* **26** 067801
[19] Fang J C, Li R J, Duan L H, Chen Y and Quan W 2015 *Rev. Sci. Instrum.* **86** 073116
[20] Pustelny S, Jackson Kimball D F, Rochester S M, Yashchuk V V and Budker D 2006 *Phys. Rev. A* **74** 063406
[21] Appelt S, Ben-Amar Baranga A, Young A R and Happer W 1999 *Phys. Rev. A* **59** 2078
[22] Jiménez-Martínez R, Griffith W C, Knappe S, Kitching J and Prouty M 2012 *J. Opt. Soc. Am. B* **29** 3398
[23] Ravishankar H, Chanu S R and Natarajan V 2011 *Eur. Phys. Lett.* **94** 53002
[24] Bell W E and Bloom A L 1961 *Phys. Rev. Lett.* **6** 280
[25] Bell W E and Bloom A L 1961 *Phys. Rev. Lett.* **6** 623
[26] Huang H C, Dong H F, Hao H J and Hu X Y 2015 *Chin. Phys. Lett.* **32** 098503
[27] Lucivero V G, Anielski P, Gawlik W and Mitchell M W 2014 *Rev. Sci. Instrum.* **85** 113108
[28] Liu G B, Li X F, Sun X P, Feng J W, Ye C H and Zhou X 2013 *J. Magn. Reson.* **237** 158
[29] Wang M L, Wang M B, Zhang G Y and Zhao K F 2016 *Chin. Phys. B* **25** 060701
[30] Seltzer S J 2008 *Developments in Alkali-Metal Atomic Magnetometry* (Ph. D. Dissertation) (New Jersey: Princeton University)
[31] Balabas M V, Budker D, Kitching J, Schwindt P D D and Stalnaker J E 2006 *J. Opt. Soc. Am. B* **23** 1001
[32] Rochester S M 2010 *Modeling Nonlinear Magneto-optical Effects in Atomic Vapors* (Ph. D. Dissertation) (Berkeley: UC Berkeley)
[33] Han R Q, Balabas M, Hovde C, Li W H, Roig H M, Wang T, Wickenbrock A, Zhivun E, You Z and Budker D 2017 *AIP Adv.* **7** 125224
[34] Auzinsh M, Budker D and Rochester S M 2010 *Optically Polarized Atoms, Understanding Light-atom Interactions* (New York: Oxford University Press) p. 190
[35] Wang M B, Zhao D F, Zhang G Y and Zhao K F 2017 *Chin. Phys. B* **26** 100701
[36] Steck D A 2010 *Cesium D Line Data* available online at http://steck.us/alkalidata [2010-12-23]
[37] Shi Y Q, Scholtes T, Grujić Z D, Lebedev V, Dolgovskiy V and Weis A 2018 *Phys. Rev. A* **97** 013419
[38] Budker D and Kimball D F 2013 *Optical Magnetometry* (Cambridge: Cambridge University Press) p. 91